EMERGING GLOBAL TRENDS IN AEOLIAN BEDFORM MOBILITY ON MARS. M. E. Banks[1], P. E. Geissler[2], N. T. Bridges[3], P. Russell[4], S. Silvestro[5,6], M. Chojnacki[7], J. R. Zimbelman[4], and W. A. Delamere[8].[1]Planetary Science Institute, Tucson, AZ, banks@psi.edu. [2] US Geological Survey, Flagstaff AZ. [3]Johns Hopkins University, Applied Physics Laboratory, Laurel, MD. [4]Center for Earth and Planetary Studies, Smithsonian Air and Space Museum, Washington, DC, [5]INAF Osservatorio Astronomico di Capodimonte, Napoli (Italy). [6]Carl Sagan Center, SETI Institute, CA, [7]Lunar and Planetary Lab, U.A., Tucson, AZ, [8]Delamere Space Sciences, Boulder, CO.

Introduction: Until relatively recently, it was not clear as to whether fields of sand dunes on Mars were actively evolving in the present martian climate [1–4]. When wind velocity exceeds the threshold speed, sand particles are mobilized. However, due to Mars' thin atmosphere, the threshold friction speed for movement of fine sand is several times greater than on Earth [e.g., 1]. The High Resolution Imaging Science Experiment (HiRISE) on Mars Reconnaissance Orbiter (MRO) has acquired sets of images covering aeolian features at resolutions up to 25 cm/pixel, and with consistent lighting conditions, at intervals of 1 or more martian years. Analysis of these repeat image sets has led to the detection of changes and the migration of aeolian bedforms (dunes and ripples) in about 70% of the locations investigated (excluding locations between 70-90° N latitude where the detection of movement was 100%), with other locations not yet revealing detectable changes or movement (Fig. 1) [e.g. 5–12].

While such imaging currently exists in only a limited number of locations, preliminary results hint at possible trends in the global distributions of active and inactive bedforms, and provide potential insight into local and regional conditions most conducive to bedform mobilization on the martian surface. Here we investigate possible emerging trends in the mobility of bedforms in relation to their general location, albedo, surrounding surface slope, and elevation.

Results and Discussion: *Spatial distribution.* Figure 1 shows the locations of bedforms analyzed for changes. Locations of transverse aeolian ridges (TARs) have not been included due to the lack of evidence for activity in current martian atmospheric conditions [e.g., 13]. The majority of observations in the northern hemisphere indicate movement. This is especially apparent in the high northern latitudes (polar erg) where all of the image pairs investigated indicated movement. Observations in the southern hemisphere show a more even distribution of results with roughly half the locations exhibiting movement and half with no detectable changes. Movement detected in the high northern latitudes may be associated with strong katabatic winds from the high elevation polar cap [14–15] and possibly with the presence of seasonal volatiles [6–7,9,14]. Bedforms at high southern latitudes may be stabilized by agents such as ground ice acting over a longer period of time in comparison to the north polar region [16].

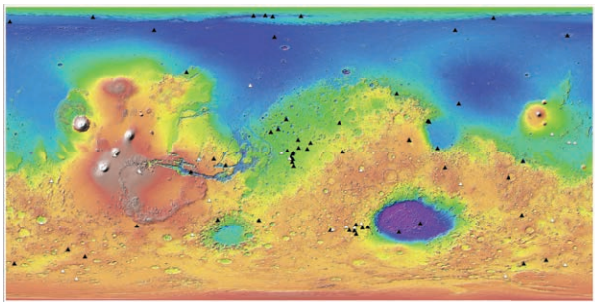

Figure 1: Locations of bedforms where movement has been detected (black triangles) and where no movement has been detected (white triangles) overlaid on Mars Orbiter Laser Altimeter topography. TARs are not included.

Bedform albedo and dust coverage. For both active and inactive bedforms, and for TARs, mean DN values were determined over small areas of representative dune surfaces with low surface slopes using HiRISE RED (570-830 nm) images. The mean DN was translated into the radiance factor (*I/F*; *I/F* = (DN * Scaling Factor) + Offset), and divided by the cosine of the solar incidence angle [17]. Images were also assessed as to the dust content of the atmosphere at the time of acquisition and outliers (i.e. offset values >0.9) were eliminated. Figure 2 shows the average albedo

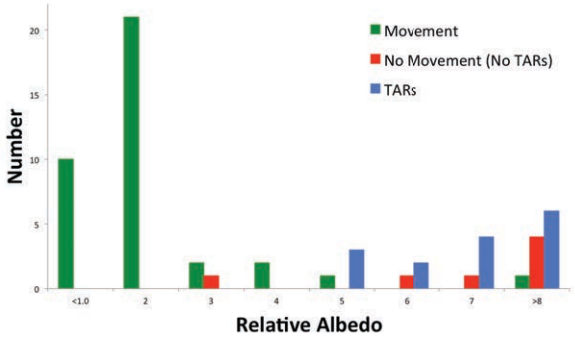

Figure 2. Average albedo signatures for different dune fields relative to the average albedo for the dunes in Nili Patera.

signature for different dune fields relative to the that of the well documented active bedforms in Nili Patera [e.g. 5]. Initial results indicate that active bedforms generally have low albedos, or dark and presumably fresh surfaces. In contrast, bedforms with no detectable movement (including TARs) generally have higher albedos. These relatively bright surfaces may be the

result of a number of processes that cause an initial mobile bedform to become immobile, such as anchoring by a coarse creep grain population or a decline in wind intensity, that then allows dust to accumulate, resulting in further stabilization [e.g., 1, 9].

Surrounding surface slopes: Average kilometer-scale surface slopes of the dune fields and immediately surrounding surfaces were calculated from profiles derived from the MOLA global base map in JMARS. Slopes associated with both active and inactive bedforms ranged from ~0.05-6°, with ~80% of the slopes ≤1°. Thus local surface slopes do not generally appear to differ for active versus inactive bedforms and likely do not play an significant role in influencing bedform mobility (with the exception of the steep slopes and high elevations in the far northern latitudes associated katabatic winds)

Dune fields located in impact craters. Roughly 70% of the dune fields located within craters exhibit detectable movement, the same percentage obtained for the dune locations analyzed outside of craters (excluding locations between 70-90° N latitude). Thus while craters serve as excellent traps for sediments, the topography associated with craters (tens of kilometers in diameter or larger) does not appear to be crucial for creating conditions conducive to bedform mobilization. However, for the craters investigated so far, a general trend is emerging in the location of active dune fields versus inactive dune fields on the crater floor. Using dune slipface orientations to derive paleowind directions, roughly 75% of inactive dune fields are centrally located or located within the upwind portion of crater floors. In contrast, 80% of the active dune fields are located in the downwind half of the crater floors, often right at the downwind crater wall (consistent with observations discussed in [18]). The significance and implications of this initial trend is unclear but may be related to the age of the dune field or maturity or duration of development.

Elevation. An estimated elevation of the dune field and immediate surrounding area was obtained from the label file for the associated HiRISE image pair (Fig. 3 and 4). The majority of the bedforms located at low elevations (-1 km and lower) are active, while the majority of bedforms at high elevations (3 km and higher) appear to be inactive. At the highest elevations in this data set (≥4 km), no observations of bedforms showed evidence of movement (Fig. 3). Higher rates of migration are also more commonly observed at lower elevations and may suggest that bedforms at higher elevations are simply migrating so slowly we are not yet able to observe the movement (Fig. 4). The slightly higher atmospheric pressure associated with lower elevations may enable bedforms to move more frequently in the denser atmosphere; threshold friction speed is inversely proportional to the square root of atmospheric density [1,8,19-21]. In the same way, the general difference in elevation of the northern lowlands/global dichotomy and the southern highlands may contribute to the greater number of active bedform detections in the northern hemisphere.

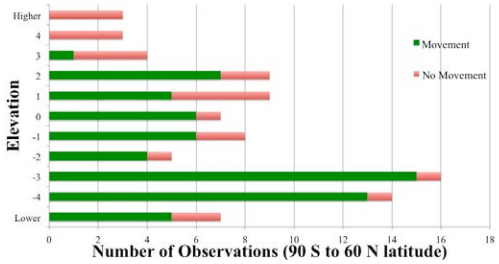

Figure 3: Number of observations per kilometer of elevation, (expressed as kilometers above the 6 mbar datum) showing movement (green) and no detectable movement (red).

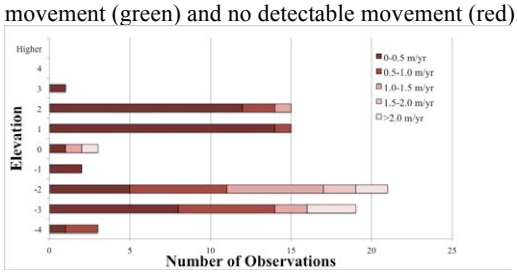

Figure 4: Distribution of rates of migration (in meters/Earth year) by elevation.

Acknowledgments: This research is supported by NASA MDAP Grant NNX14AO96G.

References: [1] Greeley R. and Iverson J. D. (1985) *Wind as a Geologic Process*, *Cambridge University Press*, 333pp. [2] Zimbelman, J. R. (2000) *GRL*, doi:10.1029/ 1999GL008399. [3] Malin, M. C., and Edgett, K. S. (2001), *JGR*, doi:10.1029/2000JE001455. [4] Bourke, M. C. et al. (2008), *Geomorph*, 94, 247-255. [5] Silvestro S. et al., (2010), *GRL*, *37*, doi:10.1029/2010GL044743. [6] Silvestro S. et al. (2011), *GRL*, *38*, doi:10.1029/ 2011GL048955. [7] Hansen, C. J. et al. (2011), *Science*, *331*, 575–578. [8] Bridges, N. T. (2012), *Geology*, *40*, 31–34. [9] Bridges, N. T., et al (2013), *Aeolian Research*, *9*, 133–151. [10] Chojnacki et al. (2011) JGR, doi:10.1029/2010JE003675, 2011 [11] Chojnacki M. et al. (2015) *This Conference*. [12] Banks et al. (2014) *LPSC*, #2857. [13] Sullivan, R. et al. (2005), *Nature*, *435*, 58–61. [14] Horgan, B. H. N. and Bell, J. F. (2012), *GRL*, *39*, doi:10.1029/ 2012GL051329. [15] Ewing, R. C. et al. (2010), *JGR*, *115*, doi:10.1029/2009JE003526. [16] Fenton, L. K. and Hayward, R. K. (2009), *Geomorphology*, *121*, 98–121. [17] Delamere, W. A. et al. (2010), *Icarus 205*, 38–52, doi:10.1016/j.icarus.2009.03.012. [18] Hayward, R. et al. (2007), *JGR*, doi:10.1029/2007JE002943 [19] Lorenz et al. (2014), *Icarus*, *230*, 77-80. [20] Chojnacki et al. (2014), *Icarus*, *230*, 96-142. [21] Hess, S. L. et al. (1980), *GRL*, *7*, 197–200.